Supplementary Information

Supplementary methods

Participants: Dysplasic Subject D1 had three residual fingers attached to the shoulder. Dysplasic Subject D2 had bilateral dysplasic malformations with completely missing upper limbs on both sides (a complete absence of arm, forearm, hand and fingers). Dysplasic Subject D3 had a shortened right arm (± 10 cm humerus). Dysplasic Subject D4 had one residual finger attached to the shoulder. The dysplasic individuals D1, D2, D3 and D4, apart from the congenitally missing hands, had a typically developed body. Dysplasic Subject D1 reported no history of prosthesis use. D2 occasionally used a wood composite prosthesis with locking elbow and hooks controlled by cables attached to leg straps from 3 to 7 years old, a wood composite prosthesis with electronic elbow and three pronged hooks controlled by micro switches in shoulder harness from 7 to 11 years old and a composite prosthesis with myoelectric elbows and cosmetic hands from 11 to 15 years old. D3 used switch-based right and left arms prostheses as a child and still uses occasionally a switch-based right arm prosthesis as an adult. D4 used myoelectric and manual prostheses five hours a day between 3 and 14 years old. All the subjects who have used prostheses report having used these prostheses mainly, if not uniquely, to pull, maintain in place or push objects but not to manipulate, and used objects for their functional use (e.g., eating with a fork) with their feet. The IDs' profiles have been reported in previous studies (see Table S1 for corresponding identification numbers).

Table S1. Identification number of IDs in the current and previous studies

Current study	Striem-Amit et al., 2017; 2018; Vannuscorps et al., 2019 (ref. 1-3)	Vannuscorps & Caramazza, 2016a (4)	Vannuscorps & Caramazza, 2016b (5)
D1	D1	D5	
D2	D2	D2	
D3	D4	D3	D5
D4	D5	D4	

Functional Imaging: The BOLD fMRI measurements were obtained in a Siemens Tim Trio 3-T scanner at the Center for Brain Science at Harvard University with a 6-channel birdcage head coil. Functional images were acquired with a T2*-weighted gradient echo EPI (GE-EPI) sequence that employed multiband RF pulses and Simultaneous Multi-Slice (SMS) acquisition (factor of 3) (3, 4). The SMS-EPI acquisitions used a modified version of the Siemens WIP 770A. We used 69 slices of 2mm thickness. The data in-plane matrix size was 108x108, field of view (FOV) 21.6cm x 21.6cm, time to repetition (TR) = 2000ms, flip angle = 80˚ and time to echo (TE) = 28ms. 3D anatomical volumes were collected using T1-weighted images using a MPRAGE T1-weighted sequence. Typical parameters were: FOV= 25.6cm X 25.6cm, data matrix: 256x256x256 (1mm iso voxel), TR=2530ms, TE=1.64, 3.5, 5.36, 7.22ms, flip angle = 7°.

Motor experiment: The motor experiment was carried out in a block design fMRI experiment. Mouth, abdomen and either side hands (for the control subjects), shoulders, and feet were moved (simple flexing/contraction movement) in separate blocks (6 s movement and 6 s rest) in randomized order

according to an auditory cue (metronome). Four flex and relax movements were performed in each block at a frequency of 0.66 Hz.

Table S2. Coordinates of the ROIs used in MVPA

	Talairach coordinate (x, y, z)
LH Motor cortex	-32, -25, 54
LH PMd	-28, -9, 55
LH preSMA	-8, 13, 33
LH SMA	-8, -12, 56
LH PMv	-48, -2, 39
LH midIPS	-33, -54, 43
LH aIPS	-45, -33, 46
LH pIPS	-16, -63, 50
LH SPOC	-6, -74, 36

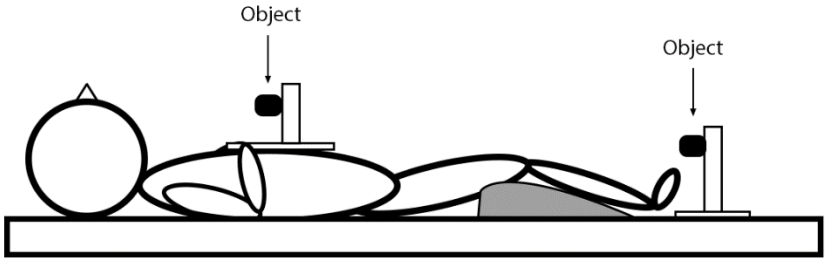

Fig. S1. Illustration of the setup in the experiment. In hand-action runs, a foam bar (1cm wide, shown in black square) mounted on a block was placed on the participant's abdomen, 30cm equidistant from both hands. In foot-action runs, the foam bar was placed in front of and equidistant (30cm) from both feet. The subjects performed a reach-to-touch or reach-to-grasp action with the instructed limb based on an auditory instruction.

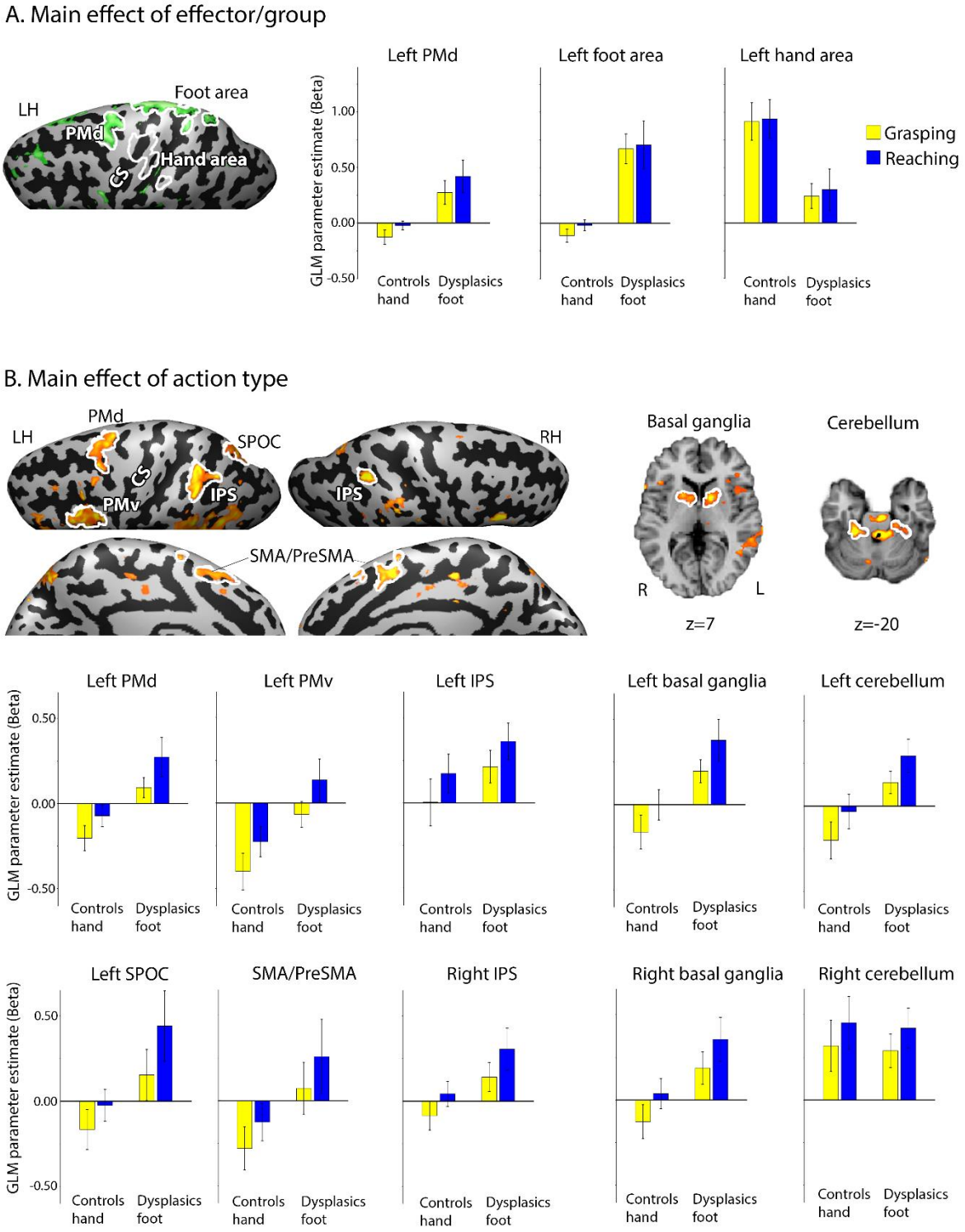

Fig. S2. Replicating **Fig. 1B, C**, the univariate RFX ANOVA with effector/group (controls' right hand and IDs' right foot) and action type (reaching, grasping) as independent variables is presented. Bar graphs plot beta values in ROIs (delineated in white). **(A)** Data sampled from brain areas with a main effect of effector/group as well as primary sensorimotor hand area. **(B)** Data sampled from brain areas with a main effect action type. No significant interaction was found.

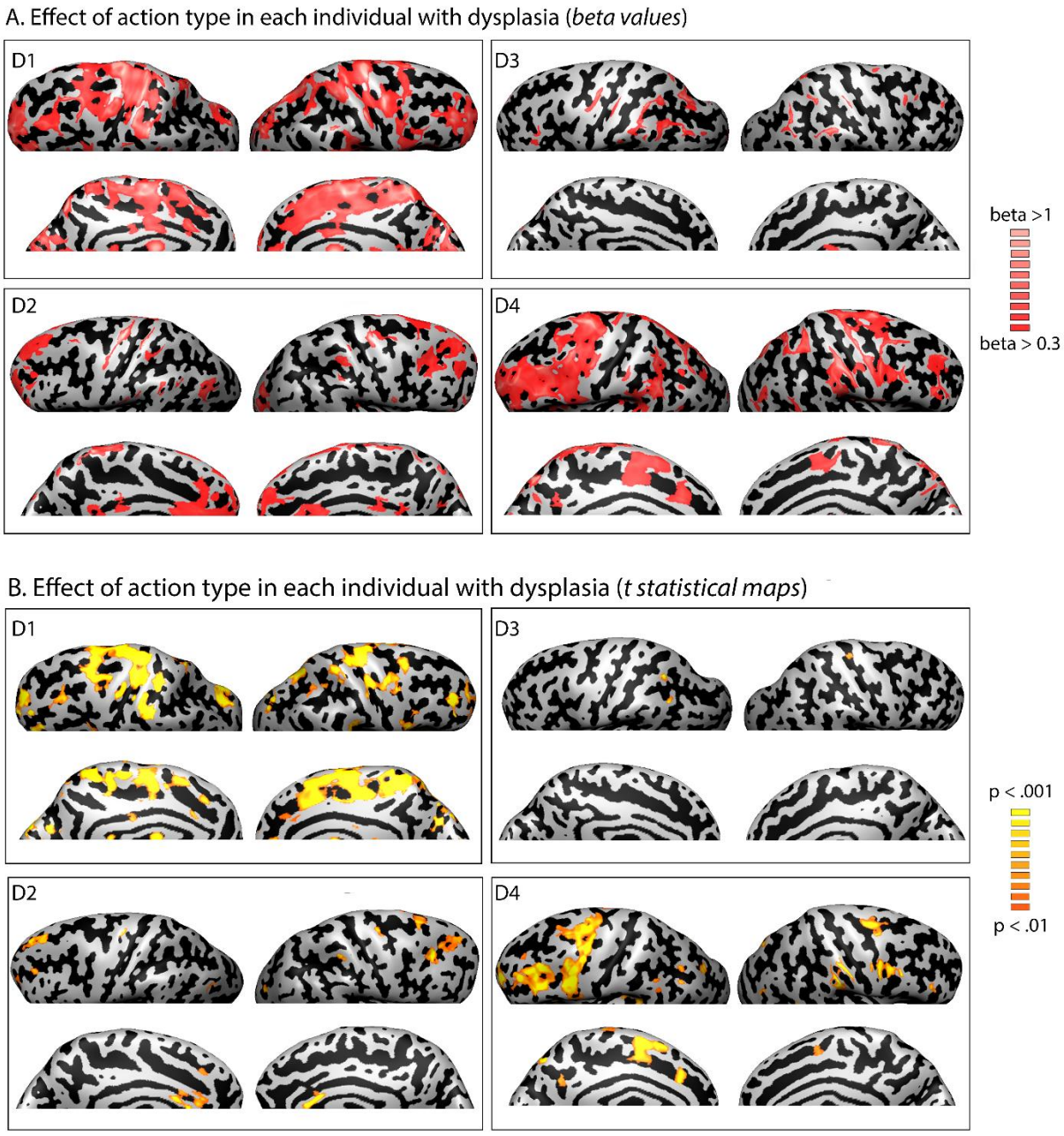

Fig. S3. The effect of action type in each individual ID, shown in A. beta values and B. t-statistical maps.

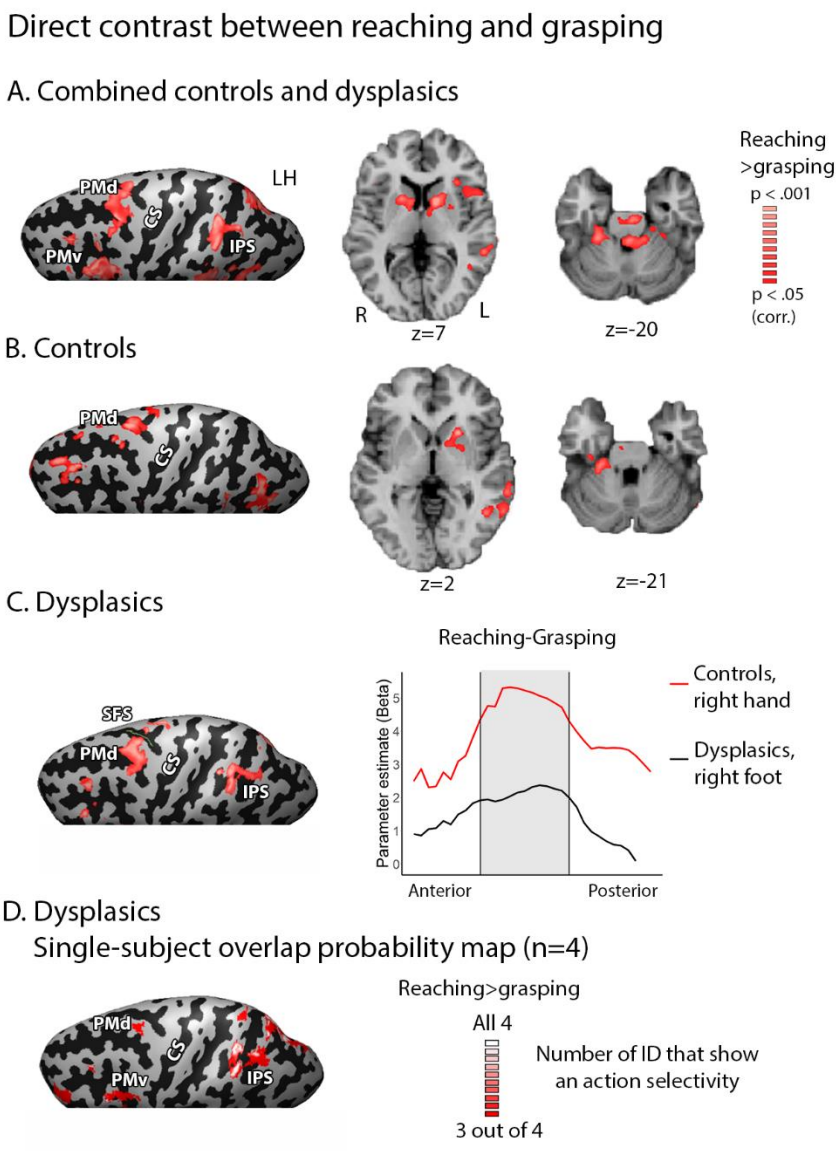

Fig. S4. Higher activation for reaching vs. grasping in areas showing a main effect of action type in univariate RFX ANOVA. **(A)** Across both groups (controls' right hand and IDs' right foot), higher activation for reaching vs. grasping was found in contralateral PMd, PMv, IPS, SPOC, and bilateral basal ganglia and anterior cerebellum. **(B)** For the controls' right hand, higher activation for reaching vs. grasping was found in left PMd, middle prefrontal cortex, basal ganglia, and right anterior cerebellum. **(C)** For the IDs' right foot, left PMd and IPS were more strongly activated by reaching vs. grasping. Line graph plots changes in the beta value of the reaching-grasping contrast along a line ROI on the SFS that demonstrates a gradient from a main effect of effector to a main effect of action type (also see **Fig. 1F**). Both groups show comparable increase in the preference for the reaching action. The gray window denotes voxels that demonstrate a main effect of action type in the univariate RFX ANOVA with effector/group (controls' right hand, IDs' right foot) and action type (reaching, grasping) as independent variables (also see **Fig. 1F**). **(D)** Single-subject overlap probability map among the IDs of areas showing higher activation for reaching vs. grasping (beta > 0.1) in PMd, PMv, and IPS.

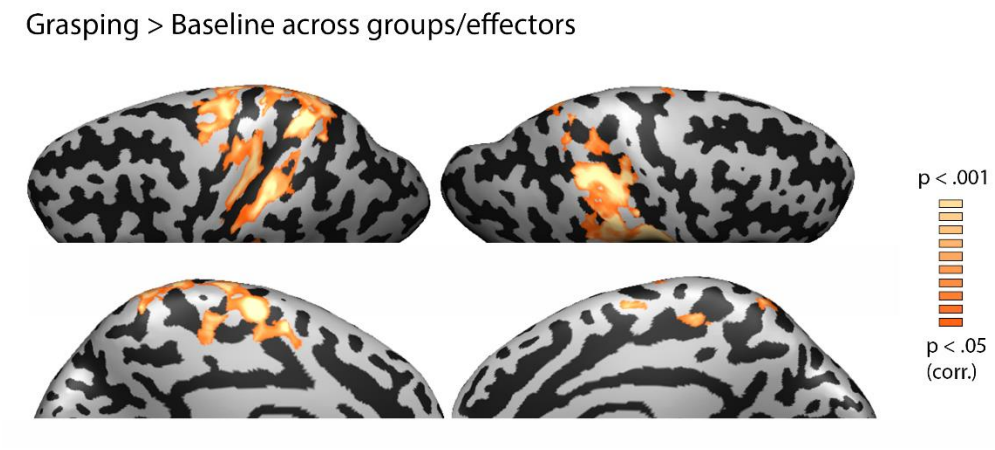

Fig. S5. Across the ID's right foot and the controls' right hand, grasping movements induced activation in primary sensorimotor cortex, premotor cortex, and intraparietal lobule and sulcus, consistent with past findings (6, 7)

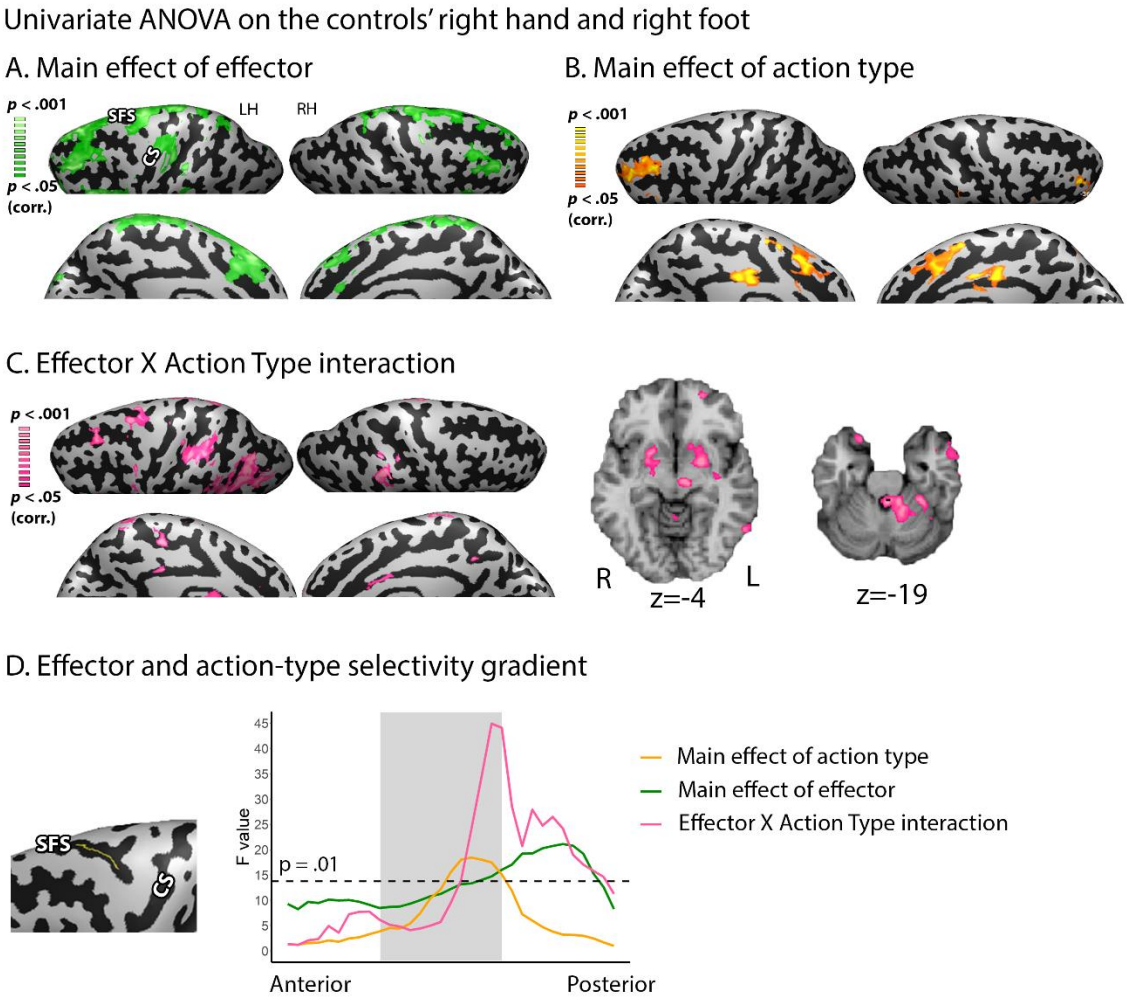

Fig. S6. Univariate RFX ANOVA with effector (controls' right hand, controls' right foot) and action type (reaching, grasping) as independent variables is displayed. **(A)** A main effect of effector was found in the primary sensorimotor area and PMd. **(B)** A main effect of action type was found in bilateral SMA/preSMA. **(C)** Brain areas with an interaction between effector and action type replicate the network showing effector-independence across groups (see **Fig. 1C**). **(D)** Although PMd does not show a significant main effect of action at the whole-brain level due to the spatial extent correction, a line graph plotting changes in the F value of each effect along a line ROI on the SFS demonstrates a gradient from a main effect of effector to a main effect of action type, mirroring the results from the controls' right hand and IDs' right foot (also see **Fig. 1E**). The gray window denotes the spatial range showing a main effect of action type for the controls' right hand and IDs' right foot. Note that here the significant (p<.01) main effect of action type falls within the same window, whereas the interaction effect peaks spatially between the two main effects.

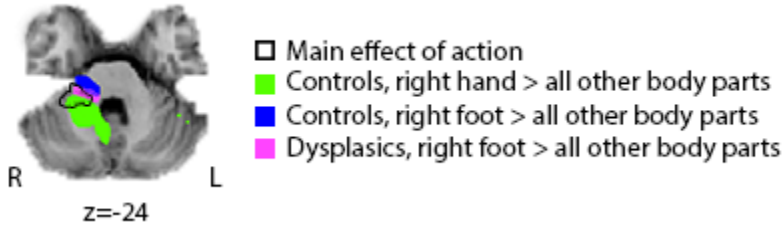

Fig. S7 Main effect of action type (reaching, grasping) in the anterior cerebellum across the controls' right hand and IDs' right foot, shown in black outline, is overlaid to a body-part-selectivity map obtained from an external motor experiment, showing the action-selective area overlaps with both effector-selective regions

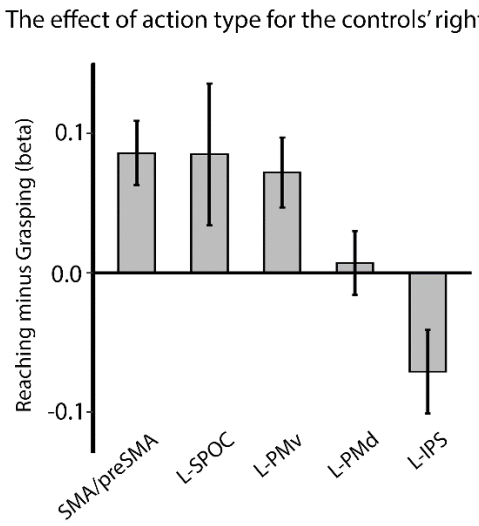

Fig. S8 Difference between reaching and grasping for the controls' right foot. In the majority of the ROIs showing a main effect of action type across the controls' right hand and IDs' right foot, similar difference between reaching and grasping was also observed for the controls' right foot. This indicates that the action-type preference was not specific to IDs due to brain reorganization and is informative of brain organization principles in typical brains.

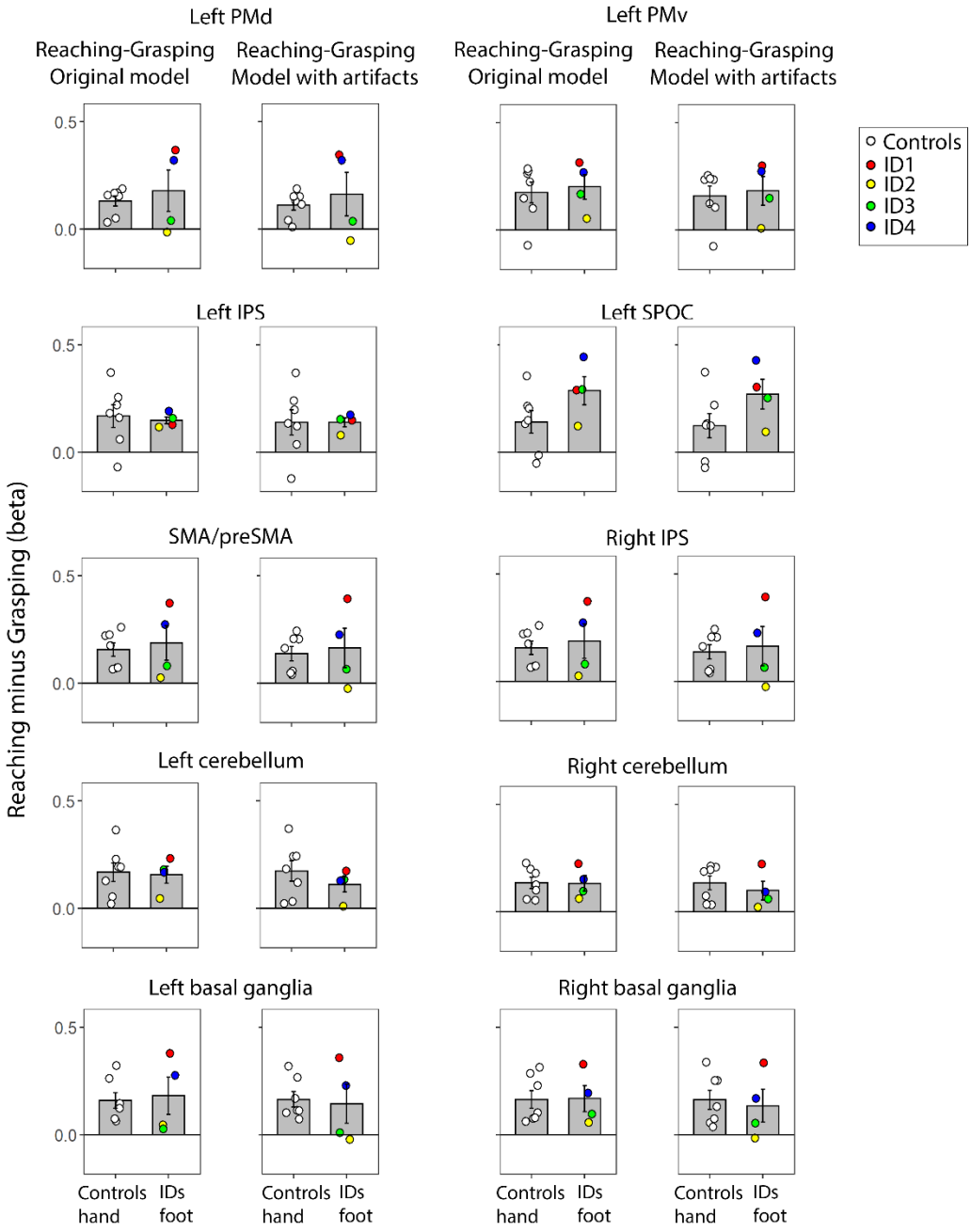

Fig. S9. Contrast between reaching and grasping when modeling potential magnetic-field-distortion artifacts resulting from limb movements. The plots show action selectivity across models in each ROI. Y-axis denotes difference in beta value between reaching and grasping (positive values denote higher activation for reaching vs. grasping). Individual subjects are denoted by circles. Figures in the first column of each ROI display results from the original model in which movement-induced artifacts were not modelled explicitly. Figures in the second column displays results when adding instantaneous (block box predictors) movement-induced artifacts as regressors. Comparing the two columns, the difference between reaching and grasping is robust to movement artifacts.

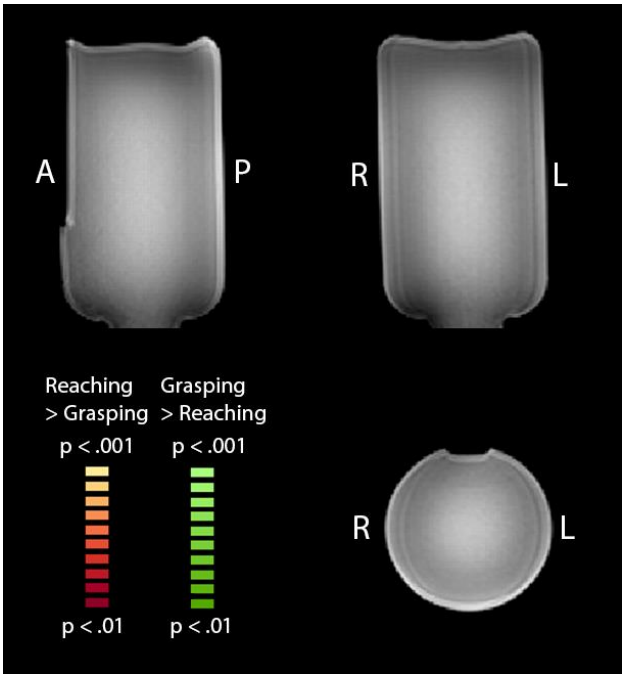

Fig. S10. To show that our core findings did not stem from magnetic field distortion artifacts due to limb movements, we repeated the experiment when a phantom was being scanned while a participant performed the reaching and grasping hand and foot actions. No differences between reaching and grasping were found on the phantom when hand and foot actions were performed in the scanner. The figure displays results at a lenient threshold of $p<0.01$ uncorrected, with the hand and foot movements collapsed. (The same null results were found considering the hand and foot movement separately.) This control experiment shows that the effect of limb movement on the magnetic field is unlikely to have caused the findings reported in the main text.

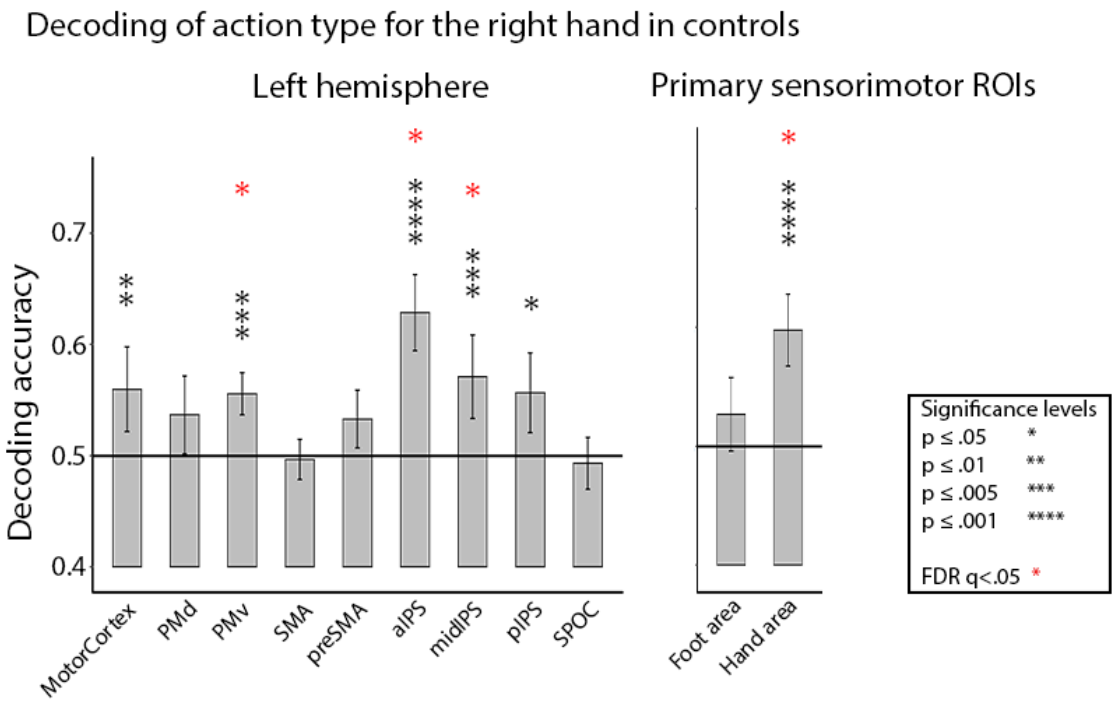

Fig. S11: **Effector-independent action-type decoding for the controls' right hand**

Decoding of action type for hand actions in the control group was significant in action peak ROIs defined in the past literature (ref. 8, Table S2) as well as in body-part selective ROIs defined from a control motor experiment. Horizontal lines at 0.5 denote chance level. Error bars denote standard error. Asterisks denote significance (red: FDR corrected for multiple comparisons).

References

1. Striem-Amit, E., Vannuscorps, G., & Caramazza, A. (2018). Plasticity based on compensatory effector use in the association but not primary sensorimotor cortex of people born without hands. Proceedings of the National Academy of Sciences of the United States of America, 115(30), 7801–7806. https://doi.org/10.1073/pnas.1803926115
2. Striem-Amit, E., Vannuscorps, G., and Caramazza, A. (2017). Sensorimotor-independent development of hands and tools selectivity in the visual cortex. Proc Natl Acad Sci U S A 114, 4787-4792.
3. Vannuscorps, G., Wurm, M., Striem-Amit, E., and Caramazza, A. (2018). Large-scale organization of the hand action observation network in individuals born without hands. Cereb Cortex 29, 3434–3444.
4. Vannuscorps, G., & Caramazza, A. (2016a). The origin of the biomechanical bias in apparent body movement perception. *Neuropsychologia*, *89*, 281-286.
5. Vannuscorps, G., & Caramazza, A. (2016b). Typical action perception and interpretation without motor simulation. *Proceedings of the National Academy of Sciences*, *113*(1), 86-91.
6. Turella, L., Rumiati, R., & Lingnau, A. (2020). Hierarchical Action Encoding Within the Human Brain. Cerebral Cortex. https://doi.org/10.1093/cercor/bhz284
7. Konen, C. S., Mruczek, R. E. B., Montoya, J. L., & Kastner, S. (2013). Functional organization of human posterior parietal cortex: Grasping- and reaching-related activations relative to topographically organized cortex. Journal of Neurophysiology, 109(12), 2897–2908. https://doi.org/10.1152/jn.00657.2012
8. Gallivan, J. P., McLean, D. A., Flanagan, J. R., & Culham, J. C. (2013). Where one hand meets the other: Limb-specific and action-dependent movement plans decoded from preparatory signals in single human frontoparietal brain areas. Journal of Neuroscience, 33(5), 1991–2008. https://doi.org/10.1523/JNEUROSCI.0541-12.2013